Restraining effect of aggregates on autogenous shrinkage in cement mortar and concrete

Lu, Tianshi; Li, Zhenming; Huang, Hao

DOI
10.1016/j.conbuildmat.2021.123166

Publication date
2021

Document Version
Final published version

Published in
Construction and Building Materials

Construction and Building Materials 289 (2021) 123166

Contents lists available at ScienceDirect

Construction and Building Materials

journal homepage: www.elsevier.com/locate/conbuildmat

Restraining effect of aggregates on autogenous shrinkage in cement mortar and concrete

Tianshi Lu [a,b], Zhenming Li [b,*], Hao Huang [b]

[a] School of Civil Engineering and Geomatics, Southwest Petroleum University, Chengdu, China
[b] Department of Materials, Mechanics, Management & Design, Faculty of Civil Engineering and Geoscience, Delft University of Technology, Delft, The Netherlands

HIGHLIGHTS

- The autogenous shrinkage of CEM I and CEM III/B mortar and concrete is studied by experiments and simulation.
- The activation energy concept is adopted to simulate the time-dependent behavior of cement paste, i.e. creep.
- The Pickett's model is extended to consider the effect of creep on the restraining effect of aggregates.

ARTICLE INFO

Article history:
Received 14 October 2020
Received in revised form 2 March 2021
Accepted 22 March 2021

Keywords:
Autogenous shrinkage
Mortar
Concrete
Creep
Restraining effect

ABSTRACT

Shrinkage-induced cracking can impair the durability of concrete structures. In the past few decades, this topic has drawn more and more attention. Shrinkage of mortar and concrete is actually the result of the interaction between the shrinking cement paste and the non-shrinking aggregates. In recent years, different models that consider the restraining effect of aggregates, i.e. Series model and Hobbs' model, have been proposed to predict the autogenous shrinkage of mortar and concrete. However, in these models both aggregate particles and cement paste matrix are considered as elastic materials. In fact, cement paste is not ideally elastic. Creep also plays an important role in autogenous shrinkage of mortar and concrete. In this paper an extended Pickett model, which takes the effect of creep into consideration, is proposed. The autogenous shrinkage of CEM I and CEM III/B cement mortar and concrete is simulated by using this model and compared with the experimental results to evaluate the accuracy of the predictions. The results show that the extended Pickett model can well predict the autogenous shrinkage of mortar and concrete.

1. Introduction

Portland cement is widely used in civil engineering since its invention in the early 19th century. The primary application of Portland cement is concrete which is made of cement paste matrix and aggregates. The focus about concrete is traditionally on the mechanical properties of the material, especially strength. In recent years, the durability of concrete structures has drawn more and more attention. Many structures need to be repaired after serving a certain period of time. Several factors affect the durability of concrete, e.g. alkali-aggregate reaction, carbonation and sulphate attack. Cracks in concrete would provide potential access for water and corrosive agents to penetrate into the concrete and accelerate the deterioration. The tensile stress induced by restrained shrinkage is one of the major reasons of cracking in concrete structures.

There are many different kinds of shrinkage, e.g. chemical shrinkage, drying shrinkage and autogenous shrinkage [1]. Among these different kinds of shrinkage, autogenous shrinkage was considered negligible for a long time. In recent years, due to the increasing utilization of high-performance concrete and ultra-high performance concrete, autogenous shrinkage becomes more and more important. Although the leading mechanism of autogenous shrinkage is still under debate, the existence of relationship between the internal relative humidity change and autogenous shrinkage is accepted by most researchers [2–7]. Surface tension, disjoining pressure and capillary tension are the three most frequently discussed mechanisms [8]. Based on these mechanisms, a few simulation models have been proposed during the past few years [5,9–11]. In these models, the autogenous shrinkage of hydrating cement paste matrix is simulated first and then the restraining effect of aggregate on the shrinking cement paste is

* Corresponding author.
E-mail address: z.li-2@tudelft.nl (Z. Li).

https://doi.org/10.1016/j.conbuildmat.2021.123166
0950-0618/

taken into consideration. Both aggregate particles and cement paste matrix are considered as elastic materials. However, the prediction of autogenous deformation by using the existing models is not satisfactory since there are always pronounced differences between the measured and calculated results after the first 24 h [5]. A few researchers thought that these differences are due to the ignorance of time-dependent behaviour of the material, i.e. creep, in these proposed models [5,12–14].

Creep is the long-term deformation of a solid material under persistent mechanical stress. The mechanism of creep has been debated during the past few decades and the most often mentioned mechanisms include seepage, viscous flow and microcracking. Although no single proposed theory describes the phenomena of creep comprehensively, the proposed mechanisms have one thing in common: they all relate to the change of microstructure and water content of the cement paste [15]. Based on the proposed mechanisms, different simulation models have been developed to predict the time-dependent behaviour of cement paste, e.g. solidification model [16]. Among these developed models, activation energy concept, which is proposed by Arrhenius in 1889 [17], has been applied by many researchers [18,19] to describe the creep behaviour of cementitious materials during the past few years.

In this paper, hydrating cement paste is dealt as visco-elastic material. The activation energy concept is adopted to simulate the time-dependent behavior of cement paste, i.e. creep. The autogenous shrinkage of cement mortar and concrete is calculated based on the autogenous shrinkage of the cement paste and the restraining effect of the aggregate particles. The restraining effect of the aggregates on the autogenous shrinkage of cement mortar and concrete is simulated by using an extended Pickett model. Pickett model [20] is a simulation model of shrinkage of concrete as a function of shrinkage of cement paste and aggregate content. Cement paste and aggregates are considered as elastic materials in Pickett model. In the extended Pickett model the effect of creep is also taken into consideration. The autogenous shrinkage of CEM I and CEM III/B cement mortar with fine sand is simulated by this model and compared with experimental results to evaluate the accuracy of the predictions. The extended Pickett model is also used to predict the early-age autogenous shrinkage of CEM I and CEM III/B concrete with coarse aggregates.

2. Methodology

2.1. Driving force of autogenous shrinkage

Cement paste is a porous material and consists of solid skeleton and pores. During the hydration process under the sealed condition, pore water is gradually consumed and internal relative humidity decreases. This phenomenon is called self-desiccation. There is a general agreement about the existence of a relationship between autogenous shrinkage and self-desiccation of the hardening cement paste. But the mechanism that causes autogenous shrinkage is still subject of debate. Surface tension, disjoining pressure and capillary tension are three most frequently discussed mechanisms. In this paper, capillary tension σ_{cap} [MPa] is adopted as the major mechanism of autogenous shrinkage which can be calculated with Laplace law [21]:

$$\sigma_{cap} = -\frac{2\gamma}{r} \tag{1}$$

where γ [N/m] is the surface tension of the pore fluid, 0.073N/m for pure water; r is the radius of the largest capillary pore still filled with water, i.e. Kelvin radius. It can be calculated as [22,23]:

$$r = -\frac{2\gamma V_w}{RTln\frac{RH}{RH_S}} \tag{2}$$

where V_w [m^3/mol] is the molar volume of water,18.02 $\times$ 10^{-6} m^3/mol; R[J/(molÂ · K)] is the ideal gas constant, 8.314 J/(molÂ · K); T[K] is the absolute temperature; RH is the measured relative humidity and RH_S reflects the effect of dissolved ions on relative humidity. In this paper, the value of RH_S is taken as 0.97 [6].

With capillary tension σ_{cap} [MPa] the internal pressure exerted by the pore water on the solid skeleton of cement paste, i.e. internal driving force of autogenous shrinkage, can be calculated by using effective stress method [24]:

$$\sigma_e = \kappa S_w \sigma_{cap} \tag{3}$$

where S_w [-] is the degree of saturation, which can be calculated as the ratio between the evaporable water content V_{ew} in the cement paste and the total pore volume V_p of the cement paste [25]:

$$S_w = \frac{V_{ew}}{V_p} = \frac{V_{iw} - V_{new}}{V_{iw} - V_{new} + V_{cs}} \tag{4}$$

where V_{iw} [cm^3 water/cm^3 paste] is the initial water content; V_{new} [cm^3 non-evaporable water/cm^3 paste] is the non-evaporable water content and V_{cs}[cm^3 chemical shrinkage/cm^3 paste] is the volume of chemical shrinkage.

κ [-] is the Biot coefficient and can be written as [26]:

$$\kappa = 1 - \frac{K_P}{K_S} = 1 - \frac{E}{3(1-2\vartheta)K_S} \tag{5}$$

where K_P [MPa] is the bulk modulus of the cement paste; K_S [MPa] is the bulk modulus of the solid skeleton of cement paste and its value can be taken as 44 GPa [27].

2.2. Autogenous shrinkage of cement paste

In this paper, the autogenous shrinkage of cement paste is divided into an elastic part and a time-dependent part:

$$\varepsilon_p(t) = \varepsilon_{el}(t) + \varepsilon_{cr}(t) \tag{6}$$

where $\varepsilon_p(t)$ [m/m] is the autogenous shrinkage of cement paste; $\varepsilon_{el}(t)$ [m/m] is the elastic part of autogenous shrinkage; $\varepsilon_{cr}(t)$ [m/m] is the time-dependent part of autogenous shrinkage, which is also called creep part.

2.2.1. Elastic part of autogenous shrinkage $\varepsilon_{el}(t)$

According to Hooke's law, the elastic part of autogenous shrinkage $\varepsilon_{el}(t)$ can be calculated as [28]:

$$\varepsilon_{el}(t) = \frac{\sigma(t)}{E(t)}(1-2\vartheta) \tag{7}$$

where $\sigma(t)$[MPa] is the internal driving force at time t;$E(t)$ [MPa] is elastic modulus of cement paste at time t; ϑ is the Poisson's ratio. In this paper, the value of Poisson's ratio of cement paste is taken as 0.2 [27].

2.2.2. Creep part of autogenous shrinkage $\varepsilon_{cr}(t)$

According to the activation energy concept [29], the work done during creep of cement paste is made up of an elastic component W_{el}, and an internal frictional component W_R:

$$Fx = W_{el} + W_R \tag{8}$$

in which F is the load that causes the deformation and x is the deformation.

Assuming Hooke's Law, the elastic component W_{el} can be expressed as:

$$W_{el} = Al\int_0^{\varepsilon} E\varepsilon d\varepsilon = AlE\frac{\varepsilon^2}{2} = Al\frac{E}{2}\frac{x^2}{l^2} = \frac{AE}{2l}x^2 \tag{9}$$

where A[m^2] and l [m] are the cross-section and length of the sample, respectively. E [MPa] is the elastic modulus.

The frictional component W_R is proportional to both $\dot{x}$ and number of points of contact in the cement gel which can be expressed as the amount of hydrated cement $\alpha C'$(C'equals the amount of initial cement per unit volume and α is the degree of hydration), then [29]:

$$W_R = R'\alpha C' x\dot{x} \tag{10}$$

Where R'R'[N/m] is a parameter of proportionality. The value of R' increases with increasing deformation. According to Wittmann [30,31], R' can be written in form of activation energy as:

$$R' = \frac{A\sigma}{\omega sinh(\eta\sigma)lN\alpha} exp(\frac{Q}{RT}) \tag{11}$$

where Q [J] is the activation energy of the cement paste; ω [-] and η [m^2/N] are structure dependent parameters and constant for a given material [32]; R [J/(mol · K)] the universal gas constant and T [K] the absolute temperature.

Inserting Equation (9) and Equation (10) in Equation (8) gives:

$$Fx = \frac{AE}{2l}x^2 + R'\alpha C' x\dot{x} \tag{12}$$

If we solve this equation, the time-dependent deformation of the cement paste specimen x is obtained [31]:

$$x(t) = \frac{2Fl}{AE}(1 - exp(-\frac{AE}{2lR'N\alpha}t)) \tag{13}$$

The time-dependent strain of the cement paste specimen can be written as [32]:

$$\varepsilon_{cr}(t) = \frac{2\sigma}{E}\left(1 - exp\left(-\frac{AE}{2lR'N\alpha}t\right)\right) \tag{14}$$

Combining Equation (11) and Equation (14), we obtain:

$$\varepsilon_{cr}(t) = \frac{2\sigma}{E}\left(1 - exp\left(-\frac{\omega sinh(\eta\sigma)E}{2\sigma exp(\frac{Q}{RT})}t\right)\right) \tag{15}$$

2.3. Restraining effect of aggregates on shrinkage of cement mortar and concrete

In order to quantify the restraining effect of aggregate particles on the shrinkage of cement mortar and concrete, an extended Pickett model is proposed in this paper. In extended Pickett model, aggregate particles are considered as elastic material and the surrounding cement paste is considered as homogeneous and viscoelastic material. The restraining effect of one spherical aggregate particle on the shrinking cement paste is calculated first. According to Pickett [20], the cement paste in the mixture is represented as one single shell surrounding the spherical aggregate particle. The restraint by the spherical aggregate particle when the surrounding cement paste tends to shrink will cause the following stresses in the large cement paste shell as shown in Fig. 1 [28,33]:

$$\sigma_r = -\frac{pa^3}{r^3}\frac{b^3 - r^3}{b^3 - a^3} \tag{16}$$

$$\sigma_t = \frac{pa^3}{2r^3}\frac{b^3 + 2r^3}{b^3 - a^3} \tag{17}$$

where σ_r [MPa] is the stress in the radial direction, σ_t [MPa] is the stress perpendicular to the radius, r [m] is the radial coordinate,

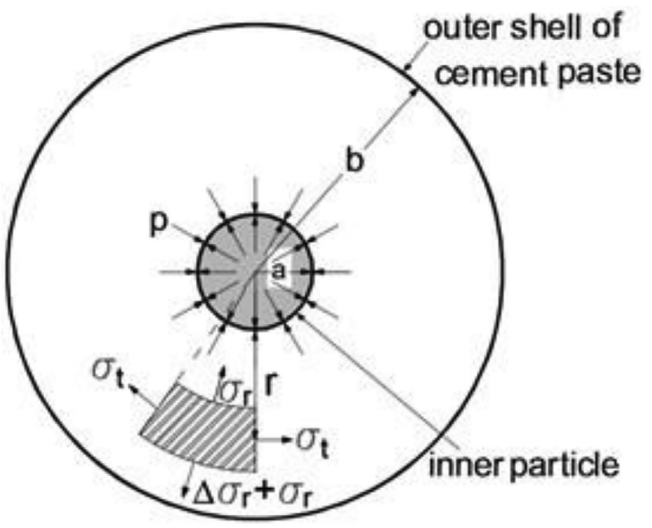

Fig. 1. Schematic illustration of a spherical aggregate particle with cement paste shell.

a[m] is the radius of the inner sphere, b[m] is the radius of the outer shell, p [MPa] is the unit pressure between inner particle and outer shell generated by the shrinkage of the outer shell.

In extended Pickett model, the change of radius δ of the outer shell (Fig. 2) caused by the restraining effect of the aggregate particle is supposed to consist of an elastic and a time-dependent parts, as shown by:

$$\delta = \delta_e + \delta_c \tag{18}$$

where δ_e is the elastic part and δ_c is creep.

For the elastic part δ_e, it holds the same as described in Pickett model [20]:

$$\delta_e = \frac{r}{E}[(1-\mu)\sigma_t - \mu\sigma_r] \tag{19}$$

The activation energy concept introduced in Section 2.2.2 is adopted to calculate the creepδ_c, which is written as:

$$\delta_c = \frac{2r}{E}[(1-\mu)\sigma_t - \mu\sigma_r]\left(1 - exp\left(-\frac{\omega sinh(\eta\sigma)E}{2\sigma exp(\frac{Q}{RT})}t\right)\right) \tag{20}$$

From Equations 16–20, the change of radius δ can be calculated as:

$$\delta = \delta_e + \delta_c = \frac{pa^3}{Er^2}\left[\frac{1-\mu}{2}\frac{b^3 + 2r^3}{b^3 - a^3} - \mu\frac{b^3 - r^3}{b^3 - a^3}\right] \times \left[1 + 2\left(1 - exp(-\frac{\omega sinh(\eta\sigma)E}{2\sigma exp(\frac{Q}{RT})}t)\right)\right] \tag{21}$$

The restraint of the aggregate particle reduces the shrinkage of the total body by the amount:

$$4\pi b^2\delta|r=b = \frac{3pV_i}{E}\left(\frac{1-\mu}{2}\right)\frac{3b^3}{b^3 - a^3}\left[1 + 2\left(1 - \exp\left(-\frac{\omega\sinh(\eta\sigma)E}{2\sigma\exp(\frac{Q}{RT})}t\right)\right)\right] \tag{22}$$

where $V_i = 4/3\pi a^3$ is the volume of the inner aggregate particle.

If there is no restraint, the surrounding cement paste shell will reduce in volume by $3\varepsilon V$, where $V[m^3]$ is the volume of the mixture and ε [m/m] is the linear shrinkage. The reduction in volume shrinkage due to restraint by the aggregate particle can be designated as $-3\Delta\varepsilon V$, where $\Delta\varepsilon$ is the reduction in the linear shrinkage:

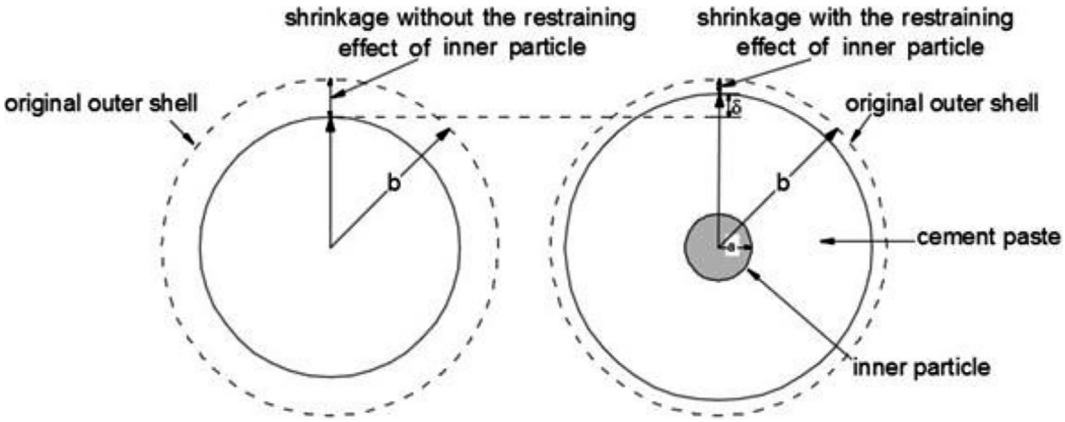

Fig. 2. Schematic representation of restraining effect of an aggregate particle on the shrinkage of cement paste.

$$-3\Delta\varepsilon V = \frac{3pV_i}{E}\left(\frac{1-\mu}{2}\right)\frac{3b^3}{b^3-a^3} \times\left[1+2\left(1-exp(-\frac{\omega sinh(\eta\sigma)E}{2\sigma exp(\frac{Q}{RT})}t)\right)\right] \quad (23)$$

Due to the shrinkage of the cement paste shell, pressure p will generate on the inner aggregate particle and this pressure will cause a volume reduction of the inner aggregate particle, which can be calculated as:

$$\frac{3(1-2\mu_i)pV_i}{E_i} = 3\varepsilon V_i - 4\pi a^2\delta|r=b \quad (24)$$

where E_i [MPa] and μ_i[−] are Young's modulus and Poisson's ratio, respectively, for the inner aggregate particle. In this paper, the values of E_i and μ_i are taken as 70 MPa [5] and 0.25 [34].

Eliminating p from Equation (23) and (24) gives:

$$-\Delta\varepsilon V = \beta\varepsilon V_i \quad (25)$$

where β is a factor which can be calculated as:

$$\beta = \frac{3(1-\mu)}{1+\mu+2(1-\mu_i)E/[1+2\left(1-exp(-\frac{\omega sinh(\eta\sigma)E}{2\sigma exp(\frac{Q}{RT})}t)\right)]E_i} \quad (26)$$

The previous text describes the restraining effect of one aggregate particle on the shrinkage of the cement paste shell. The restraining effect of all aggregate particles in the cement mortar and concrete on the shrinkage can be calculated with the following formulas. Let the volume of aggregate per unit volume of mix be g. The increase in g due to the addition of one particle of volume V_i to the mixture will be:

$$\Delta g = \frac{gV+V_i}{V+V_i} - g = (1-g)\frac{V_i}{V+V_i} \quad (27)$$

Combining Equation (25) and (27) results in:

$$\frac{\Delta\varepsilon}{\varepsilon} = -\frac{\beta\Delta g}{1-g}\frac{V+V_i}{V} \approx -\frac{\beta\Delta g}{1-g} \quad (28)$$

In differential form,

$$\frac{d\varepsilon}{\varepsilon} = -\frac{\beta dg}{1-g} \quad (29)$$

Then integrate it,

$$\varepsilon_t = \varepsilon_p(1-g)^\beta \quad (30)$$

where ε_t is the shrinkage of mortar and concrete, ε_p is the shrinkage of corresponding paste.

2.4. Simulation model of autogenous shrinkage of cement mortar and concrete

In the proposed model, early-age properties of cement paste, i.e. non-evaporable water content, chemical shrinkage, internal relative humidity and elastic modulus should be obtained by experiments as inputs. With these measured properties, the autogenous shrinkage of hardening cement paste is calculated first. Based on the calculated autogenous shrinkage of hardening cement paste, the autogenous shrinkage of cement mortar and concrete is predicted by using the extended Pickett model. In Fig. 3, a flow chart of the whole calculation procedure is shown.

2.5. A comparison between the original picket model and the extended Pickett model

Fig. 4 shows the autogenous shrinkage of blast furnace slag cement mortars (CEM III 42.5 N) with water-cement ratio 0.3 and different sand-cement weight ratio, i.e. 0.1, 0.3, 0.5 and 0.7, calculated with the original Pickett model and the extended Pickett model. This figure shows that the autogenous shrinkage calculated with the extended Pickett model is smaller than that with the original Pickett model. The difference between the calculated autogenous shrinkage with Pickett's model and the extended Pickett model of cement mortar increases with increasing sand content. For example, due to creep the calculated autogenous shrinkage of a BFS cement mortar with water-binder ratio 0.3 and sand-cement weight ratio 0.7 at 7 days changes from 180 μstrain to 120 μstrain, so decreasing by 60 μstrain (yellow dotted line and yellow solid line in Fig. 4). This is in line with results reported by Grasley [12], who studied the autogenous shrinkage of fly ash concrete with water-binder ratio of 0.33. The fly ash dosage in blended mixtures was 35% by weight of the binder. The sand-cement weight ratio was 0.74. According to Grasley [12], by taking creep into consideration, the calculated autogenous shrinkage of concrete at 10 days changed from 144 μstrain to 94 μstrain, decreasing 50 μstrain.

3. Prediction of autogenous shrinkage of cement mortar

3.1. Mixture design

The materials used to synthesize mortar were Portland cement (CEM I 42.5 N) and blast furnace slag (BFS) cement (CEM III/B 42.5 N), water and quartz sand. The Portland cement had a calculated Bogue composition of C_3S 67.1%, C_2S 5.9%, C_3A 7.8%, and C_4AF 9.6%. The mean particle size D_{50} of Portland cement and BFS

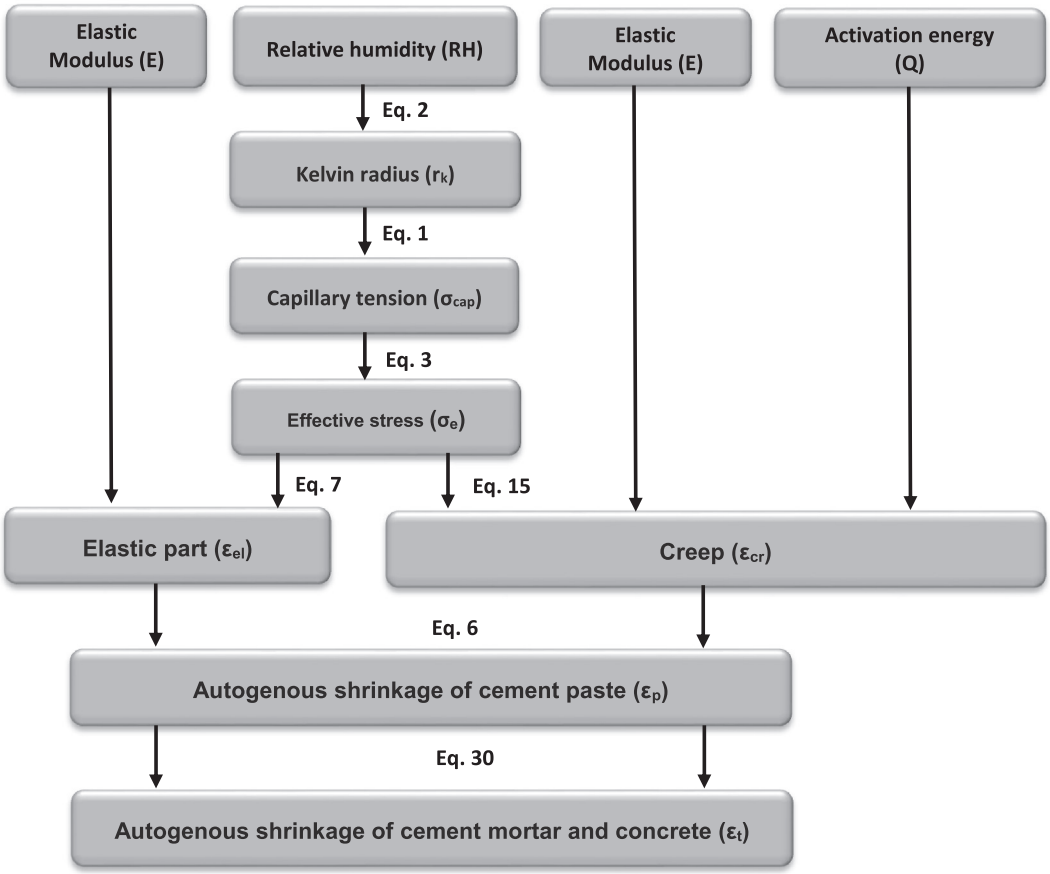

Fig. 3. Scheme of simulation model of autogenous shrinkage.

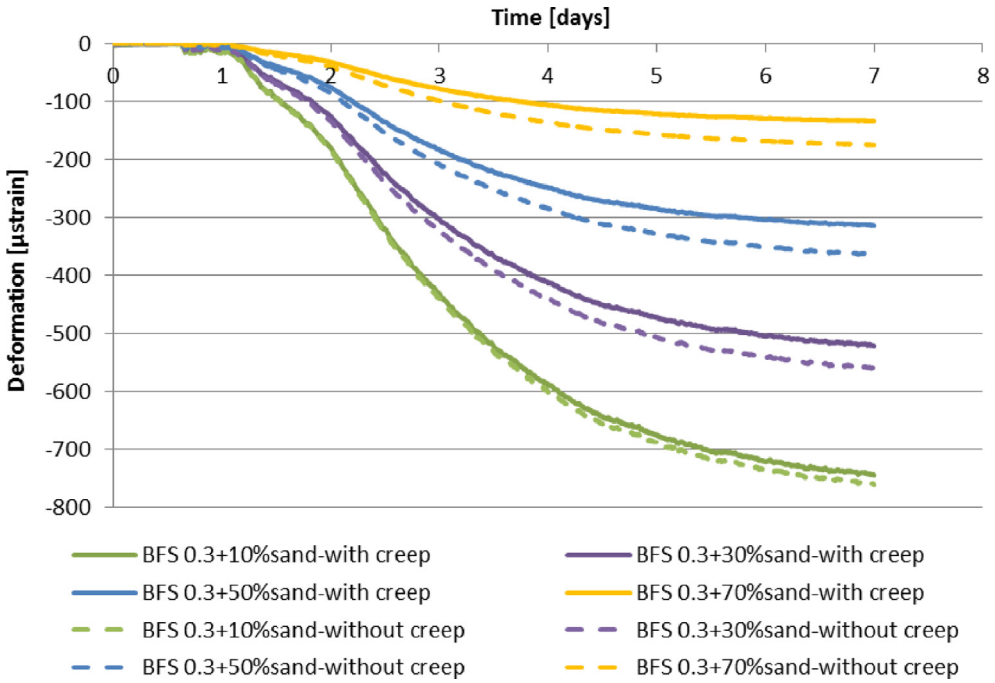

Fig. 4. Calculated autogenous deformation of BFS cement paste and mortar (sand-cement weight ratio is 0.1, 0.3, 0.5 and 0.7) with Pickett model and the extended Pickett model with water-binder ratio of 0.3.

cement were 22 μm and 24 μm, respectively. Quartz sand with size of 0.125 ~ 0.250 mm was added.

Eight mortar mixtures were utilized to study the autogenous shrinkage of cement mortar. The Portland cement pastes were

made with CEM I 42.5 N and CEM III/B 42.5 N was used to prepare slag cement pastes. In both cases, the water-binder ratios were 0.3 and 0.4. The mortars were made of the same pastes, with the sand-cement weight ratios 0.1 and 0.3. The mixture compositions of pastes and mortars are listed in Table 1. Mortar was mixed in a 5lL epicyclical Hobart mixer. The mixing process followed ASTM 305-99 [35].

3.2. Experimental methods and results

In order to calculate the autogenous shrinkage of cement paste mortar by using the proposed model, several early-age properties of cement paste need to be measured. The early-age properties of cement paste include non-evaporable water content, chemical shrinkage, internal relative humidity and elastic modulus. These measured early-age properties of Portland and BFS cement pastes can be found in a previous study [36] and are not presented in this paper.

In order to measure the autogenous shrinkage, cement paste and mortar were cast under vibration into corrugated plastic molds as shown in Fig. 5(a) (low-density polyethylene plastic, LDPE) [37]. The length and diameter of the samples were approximately 430 mm and 29 mm, respectively. After final setting time, when a solid skeleton of cement paste and mortar was formed, the measurements of autogenous shrinkage started. In this study, the final setting time was determined by the Vicat method according to standard NEN-EN 196-3:2005 [38]. The samples were placed in a glycol bath (as show in Fig. 5(b)). The temperature of the glycol bath was kept at 20 ℃. The longitudinal deformation was measured by a TRANS-TEK 350-000 displacement transducer with a measurement accuracy of ± 5 μm/m. Three specimens were tested for each measurement. Autogenous deformation of the specimens was recorded every 5 min.

Figs. 6 and 7 show the measured autogenous deformations of Portland and BFS cement pastes and mortars with water-binder ratio 0.3 and 0.4. The starting time of the measurements is the final setting time. From Figs. 6 and 7 it can be noticed that the autogenous shrinkage of cement mortars decreases with the increasing sand dosage. This phenomenon is due to the restraining effect of sand which will be numerically simulated in the following section. (Note: Deformation [μstrain] in Figures means Autogenous strain and the unit is [μm/m]).

3.3. Numerical simulation of autogenous shrinkage of cement paste and mortar

Based on the measured early-age properties of cement paste, the materials parameters include degree of saturation, capillary tension and elastic modulus are calculated firstly. Then the autogenous shrinkage of cement paste and mortar is calculated with these parameters by using the proposed model. The calculated degree of saturation, capillary tension and elastic modulus of cement paste can be found in [36]. The calculated autogenous shrinkage of cement paste can also be found in [36] and is shown in this paper as reference.

3.3.1. Portland cement paste and mortar with w/b ratio 0.3

Fig. 8(a) shows the measured and calculated autogenous shrinkage of Portland cement pastes with water-binder ratio 0.3 after the final setting time. A fast measured shrinkage can be noticed after final setting. This fast shrinkage is followed by a short period of swelling after which the specimens shrink steadily. According to some researchers [39–42] taking the final setting time as the starting point of autogenous shrinkage is questionable and the fast measured shrinkage cannot be counted into autogenous shrinkage [36]. The time when the maximum (macroscopic) swelling is observed is taken as the starting time of autogenous shrinkage in this paper [43]. In Fig. 8(b), autogenous shrinkages of Portland cement paste with water-binder ratio 0.3 after the short period of swelling are presented.

Fig. 9(b) and Fig. 10(b) show the calculated and measured autogenous shrinkage of the Portland cement mortars with water-binder ratio of 0.3 and sand-cement weight ratio 0.1 and 0.3 after the short period of swelling. The calculated contributions of elastic and time-dependent part of autogenous shrinkage are also shown in these figures. It can be noticed that the creep plays an important role in autogenous shrinkage of cement mortar and should not be neglected. This result is in line with the finding reported by Lura [5].

Figs. 9 and 10 also show the autogenous shrinkage of cement mortar with higher sand-cement weight ratio is smaller than that of cement mortar with lower sand-cement weight ratio. This is due to the restraining effect of sand on shrinking cement mortar and the effect can be simulated by using the extended Pickett model.

3.3.2. Portland cement paste and mortar with w/b ratio 0.4

Fig. 11 shows the measured and calculated autogenous shrinkage of Portland cement pastes with water-binder ratio 0.4 [36].

Fig. 12(b) and Fig. 13(b) show the calculated and measured autogenous shrinkage of the Portland cement mortars with water-binder ratio of 0.4 and sand-cement weight ratio 0.1 and 0.3 after the short period of swelling. By comparing Fig. 12(b) and Fig. 13(b) with Fig. 9(b) and Fig. 10b), it can be noticed that creep plays a more important role in autogenous shrinkage of cement mortars with high water-binder ratio. This is due to the lower stiffness of Portland cement mortar with higher water-binder ratios. The Cement mortar with lower stiffness normally

Table 1
Mixture composition of different cement pastes and mortars (% by weight).

Paste/mortar mixture name	Binder			Sand (%)
	w/b	CEM I 42.5 N (%)	CEM III/B 42.5 N (%)	
OPC 0.3	0.3	100	0	0
OPC 0.3 + 10%sand	0.3	90	0	10
OPC 0.3 + 30%sand	0.3	70	0	30
OPC 0.4	0.4	100	0	0
OPC 0.4 + 10%sand	0.4	90	0	10
OPC 0.4 + 30%sand	0.4	70	0	30
BFS 0.3	0.3	0	100	0
BFS 0.3 + 10%sand	0.3	0	90	10
BFS 0.3 + 30%sand	0.3	0	70	30
BFS 0.4	0.4	0	100	0
BFS 0.4 + 10%sand	0.4	0	90	10
BFS 0.4 + 30%sand	0.4	0	70	30

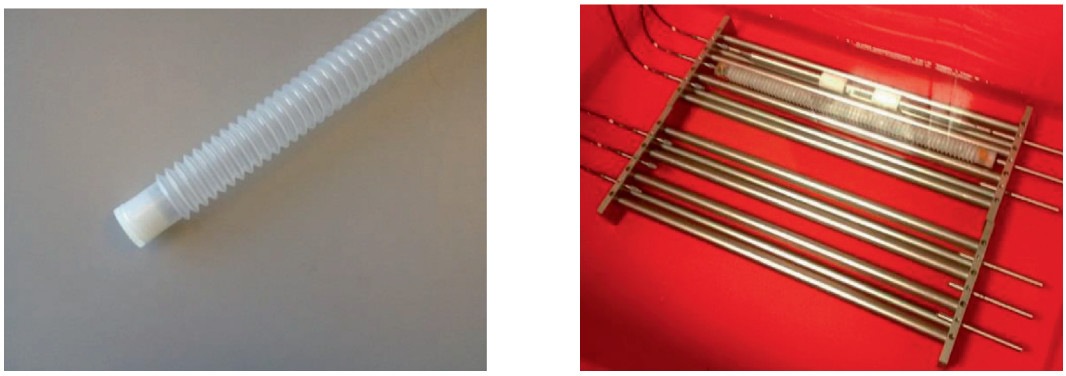

(a) corrugated plastic tube (b) glycol bath

Fig. 5. The setup for the autogenous shrinkage measurement.

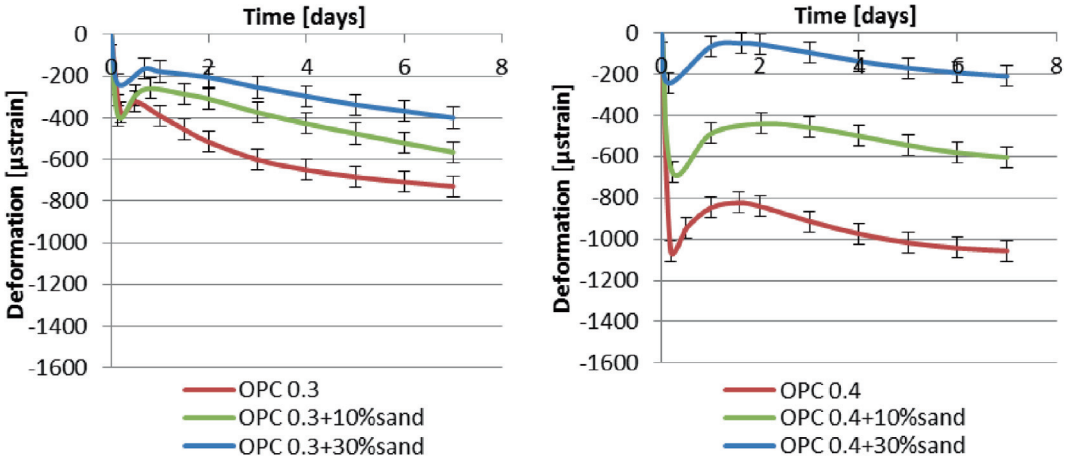

(a) Water-binder ratios of 0.3 (b) Water-binder ratios of 0.4

Fig. 6. Autogenous deformation of Portland cement paste and mortar with water-binder ratio of 0.3 and 0.4.

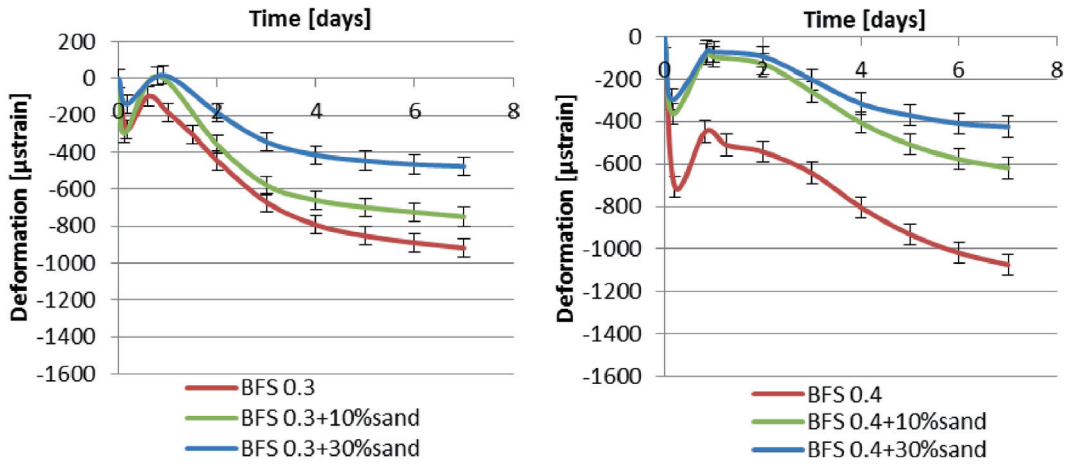

(a) Water-binder ratio of 0.3 (b) Water-binder ratio of 0.4

Fig. 7. Autogenous deformation of BFS cement paste and mortar with water-binder ratio of 0.3 and 0.4.

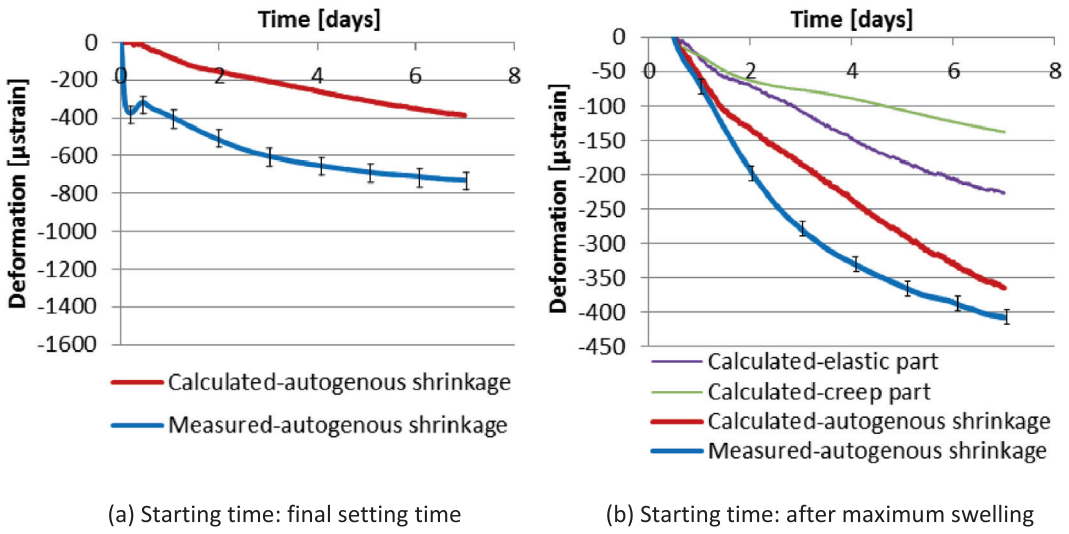

(a) Starting time: final setting time (b) Starting time: after maximum swelling

Fig. 8. Measured and calculated autogenous deformation of Portland cement paste with water-binder ratio 0.3 [36].

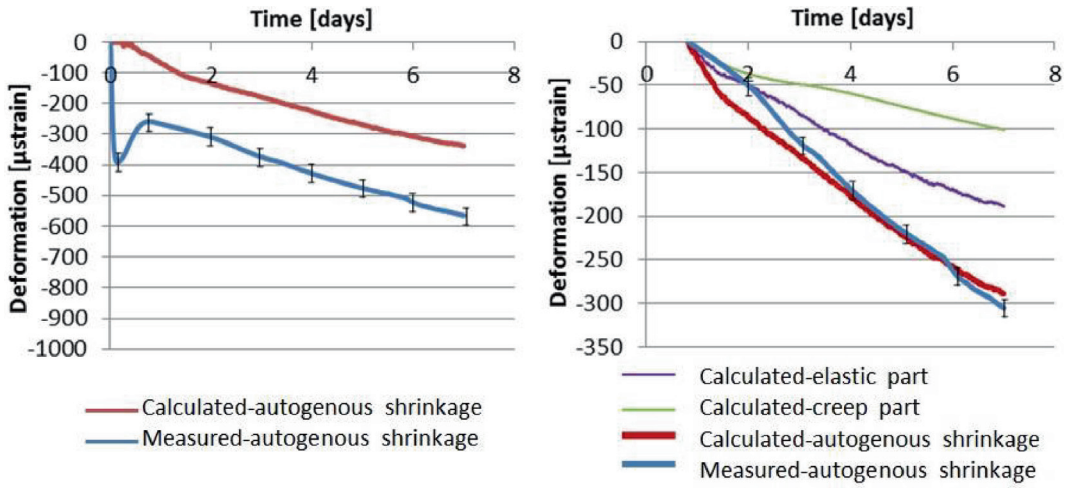

(a) Starting time: final setting time (b) Starting time: after maximum swelling

Fig. 9. Measured and calculated autogenous deformation of Portland cement mortar (10% sand) with water-binder ratio 0.3.

has a bigger creep coefficient due to the higher porosity [44]. Similar result can be found in Hu's thesis [45].

3.3.3. BFS cement paste and mortar with w/b ratio 0.3

Fig. 14 shows the measured and calculated autogenous shrinkage of BFS cement pastes with water-binder ratio 0.3 [36]. Figs. 15 and 16 show the calculated and measured autogenous shrinkage of the BFS cement mortars with water-binder ratio of 0.3 and sand-cement weight ratio 0.1 and 0.3.

The calculated autogenous shrinkage of BFS cement mortar after maximum swelling is shown in Fig. 15(b) and Fig. 16(b), divided into an elastic part and a creep part. The calculated autogenous shrinkage of BFS cement mortar is much bigger than that of Portland cement mortar with the same water-binder ratio at the same curing age (See Figs. 9 and 10). The bigger calculated autogenous shrinkage of BFS cement paste may have two reasons, i.e. lower elastic modulus and bigger capillary tension of BFS cement paste [36].

3.3.4. BFS cement paste and mortar with w/b ratio 0.4

Fig. 17 shows the measured and calculated autogenous shrinkage of BFS cement pastes with water-binder ratio 0.4 [36]. Figs. 18 and 19 show the calculated and measured autogenous shrinkage of the BFS cement mortars with water-binder ratio of 0.4 and sand-cement weight ratio 0.1 and 0.3.

The calculated autogenous shrinkage of BFS cement mortar after maximum swelling is shown in Fig. 18(b) and Fig. 19(b), including an elastic part and a creep part. It can noticed that the difference between the measured and calculated autogenous shrinkage at the first several days is big but the autogenous shrinkage at seven days is predicted well with the model. For BFS cement paste with water-binder ratio of 0.4, the relative humidity is close to 100% [36] and the measuring equipment of relative humidity is not very sensitive at that range. This may lead to a smaller measured drop of relative humidity at the first several days, which will result in smaller calculated autogenous shrinkage of cement paste and mortar.

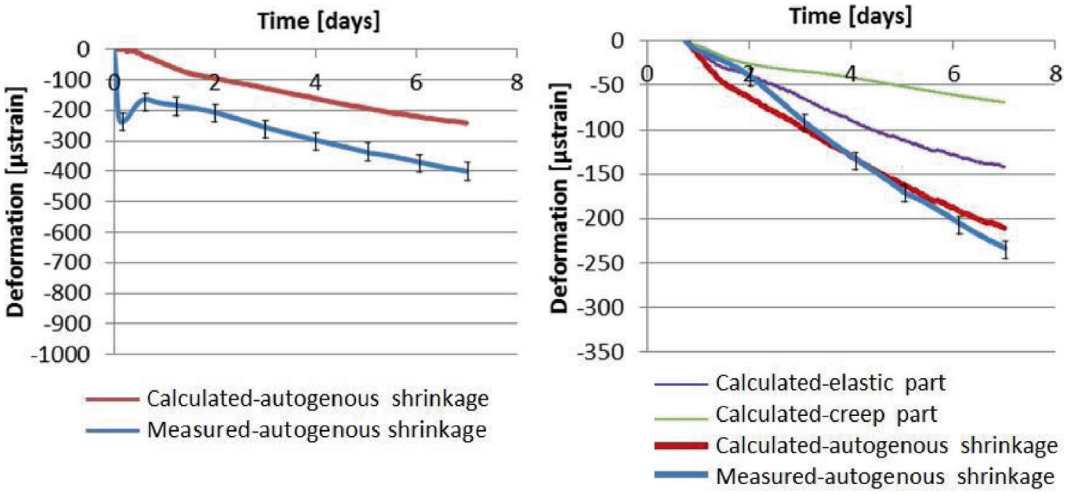

(a) Starting time: final setting time (b) Starting time: after maximum swelling

Fig. 10. Measured and calculated autogenous deformation of Portland cement mortar (30% sand) with water-binder ratio 0.3.

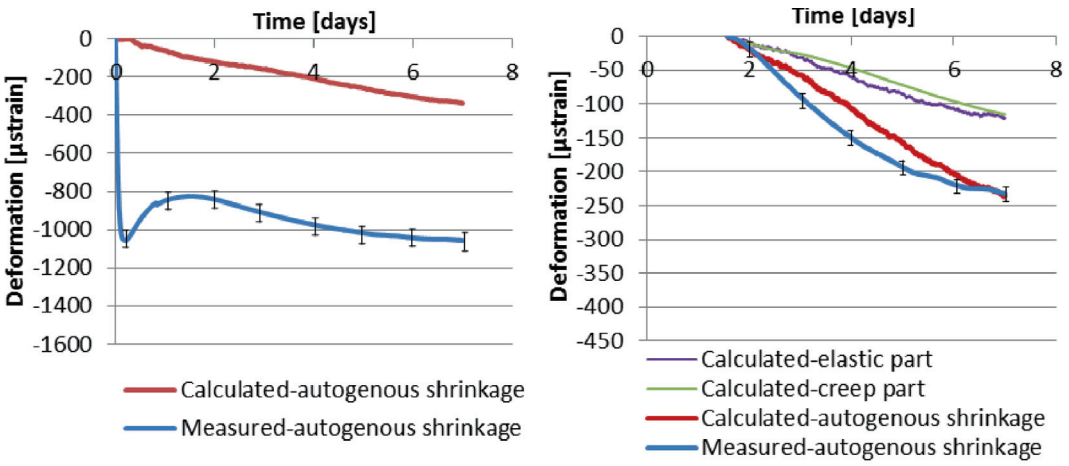

(a) Starting time: final setting time (b) Starting time: after maximum swelling

Fig. 11. Measured and calculated autogenous deformation of Portland cement paste with water-binder ratio 0.4 [36].

4. Prediction of autogenous shrinkage of concrete

In previous section the extended Pickett model was used to predict the autogenous shrinkage of cement mortar with a relatively low aggregate content (lower than 30%). In this section, Portland and BFS concretes were studied to check whether the autogenous shrinkage of mixtures with gravels and high aggregate fraction can also be accurately predicted.

4.1. Mixture design

Portland cement concrete and BFS concretes are considered for studying the autogenous shrinkage of concrete. The measured autogenous shrinkage of Portland cement concrete is taken from Zhang's paper [46]. The concrete was made with Type I (ASTM) normal Portland cement. The water-binder ratio was 0.3. The coarse aggregate used was crushed granite with a maximum size of 20 mm. The fine aggregate used was natural sand. The density of both the coarse and fine aggregates was 2650 kg/m^3. The volume fraction of aggregate of concrete is 71%. The measured autogenous shrinkages of the BFS concrete are taken from Mors [47]. The BFS concretes were made with CEM III/B 42.5 N. The water-binder ratio was 0.44 and 0.5. The fine aggregate used was sand with size of 0–4 mm. The coarse aggregate used was gravel with size 4–8 mm and 8–16 mm. The volume fraction of aggregate of concrete was 70%. The mixture compositions of Portland cement concrete and BFS concretes are listed in Table 2.

4.2. Portland cement-based concrete

4.2.1. *Experimental measurement of autogenous shrinkage (by Zhang [46])*

The concrete was mixed in a laboratory pan mixer. The fine and coarse aggregates were mixed first, followed by the addition of cement, mixing and adding water. Two specimens of 400×100×100 mm were cast for measuring the total shrinkage. The strain transducers were embedded in the concrete prism and connected to a computer-controlled data logger right after casting of the concrete specimen. Immediately after casting, each prism was sealed for the entire period of the experiment. The weight

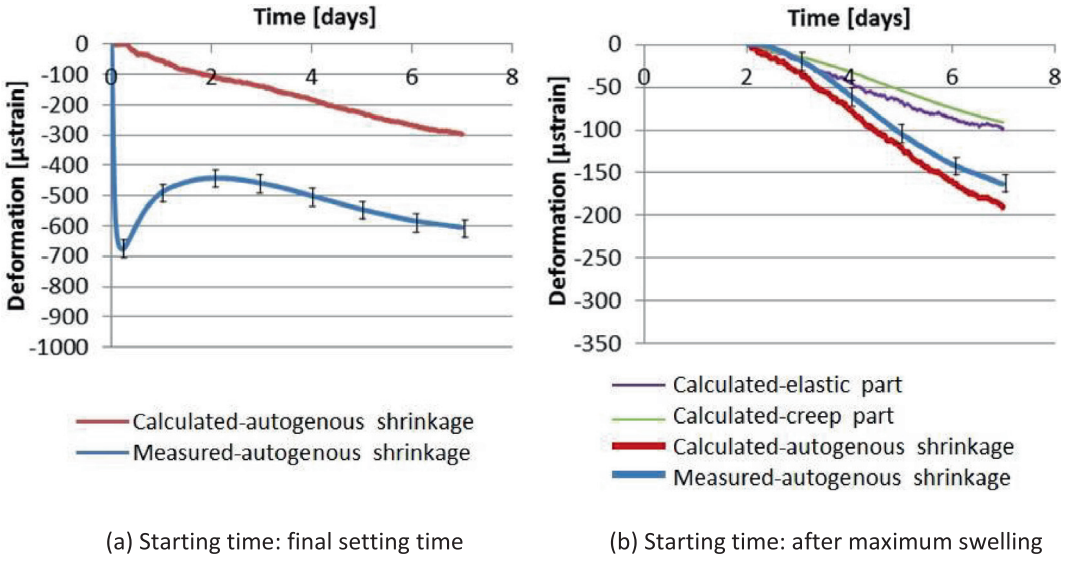

(a) Starting time: final setting time (b) Starting time: after maximum swelling

Fig. 12. Measured and calculated autogenous deformation of Portland cement mortar (10% sand) with water-binder ratio 0.4.

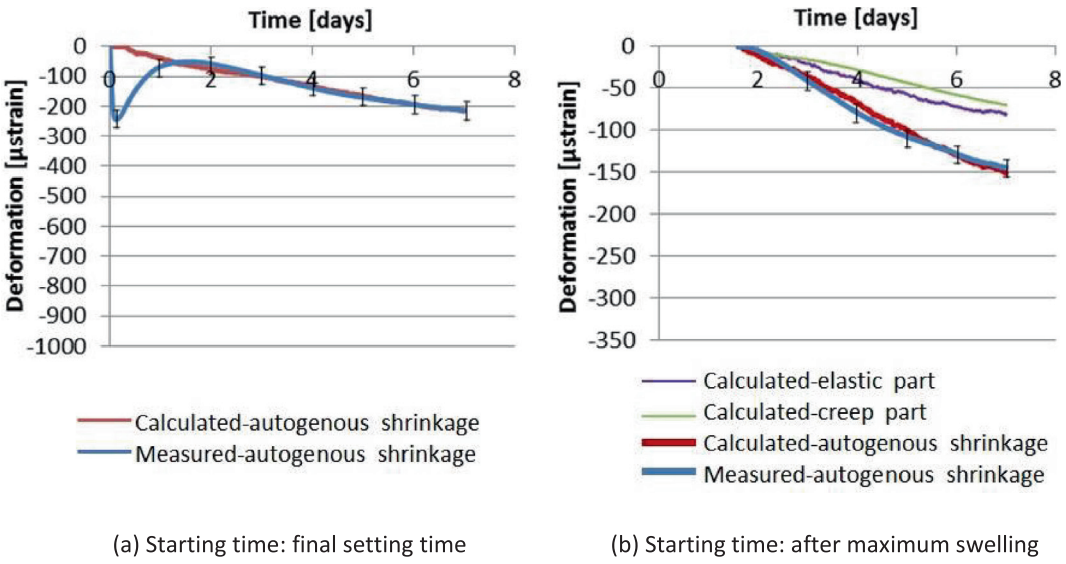

(a) Starting time: final setting time (b) Starting time: after maximum swelling

Fig. 13. Measured and calculated autogenous deformation of Portland cement mortar (30% sand) with water-binder ratio 0.4.

change of each prism was measured. The autogenous shrinkage was measured during 28 days after casting and shown in Fig. 22.

4.2.2. Numerical simulation of autogenous shrinkage

In order to simulate the autogenous shrinkage of the Portland cement concrete with the extended Pickett model, the needed parameters, i.e. the relative humidity, degree of saturation and elastic modulus of the concrete, are simulated with HYMOSTRUC [48]. In HYMOSTRUC, the degree of hydration α of cement is simulated as a function of the particle size distribution and of the chemical composition of the cement, the water/cement ratio and the reaction temperature. The relative humidity and degree of saturation of the concrete are simulated based on the degree of hydration α. Elastic modulus is calculated using the composite model [49]. Capillary tension is calculated from the simulated relative humidity using Kelvin equation (Equation (1)). The calculated results are shown in Figs. 20 and 21. The calculated autogenous shrinkage of Portland cement concrete is shown in Fig. 22. The contributions of both the elastic and time-dependent part of autogenous deformation to autogenous shrinkage are shown.

Fig. 22 shows that the prediction of the autogenous shrinkage of Portland cement concrete with the extended Pickett model is in very good agreement with the measurements. Fig. 22 also shows that the elastic part of autogenous shrinkage is almost constant after the first 14 days. After the first 14 days the creep part still increases with time and plays a more and more important role in autogenous shrinkage.

4.3. Blast furnace slag concrete

4.3.1. ***Experimental measurement of autogenous shrinkage (by Mors** [47]**)***

Two prisms of 400×100×100 mm were cast for measuring the autogenous shrinkage. After demoulding the prisms are directly wrapped in plastic foil and sealed with aluminium foil to prevent moisture exchange with the surrounding environment. A dial gauge was attached at two opposite sides of the prism to measure

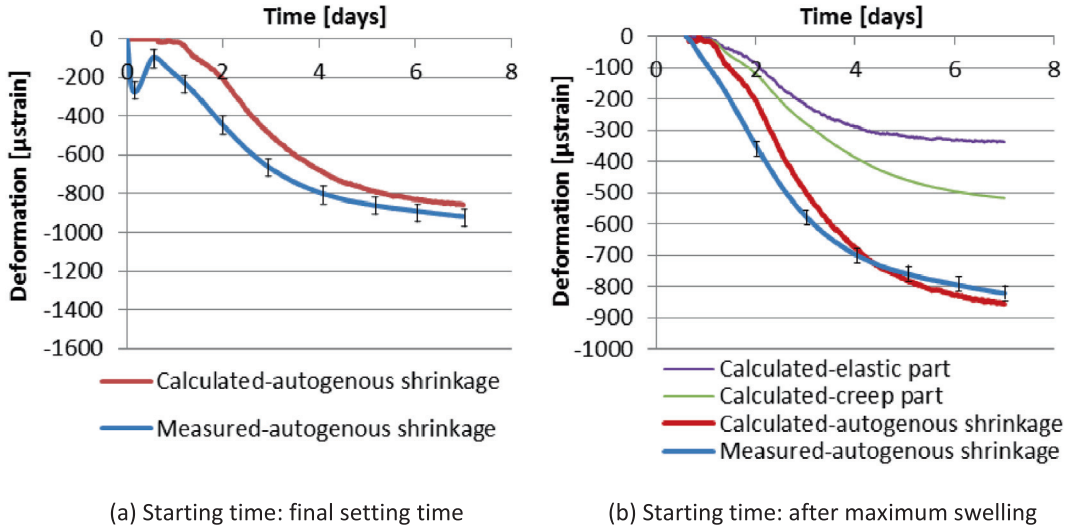

(a) Starting time: final setting time (b) Starting time: after maximum swelling

Fig. 14. Measured and calculated autogenous deformation of BFS cement paste with water-binder ratio 0.3 [36].

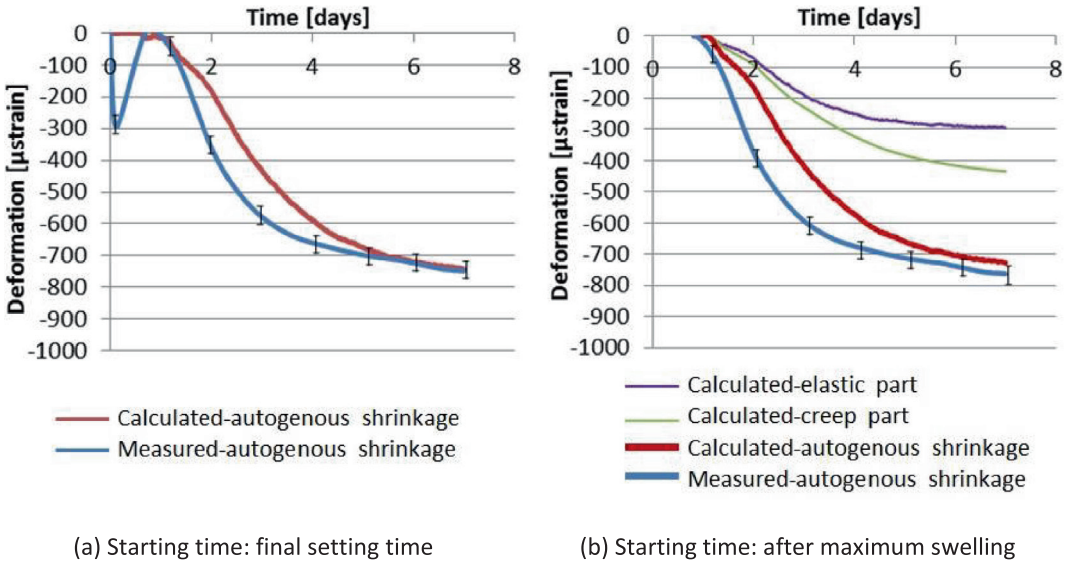

(a) Starting time: final setting time (b) Starting time: after maximum swelling

Fig. 15. Measured and calculated autogenous deformation of BFS cement mortar (10% sand) with water-binder ratio 0.3.

the autogenous shrinkage. The measuring length of the dial gauge is 20 cm and the accuracy of the dial gauge is 1 μm. The weight loss of each prism was measured. The measured weight loss was used to correct the autogenous shrinkage measurement for minor leakage through the sealing. The corrected autogenous shrinkage of BFS concrete with water-binder ratio 0.44 and 0.5 are shown in Figs. 25 and 26.

4.3.2. Numerical simulation of autogenous shrinkage

The calculated autogenous shrinkage of BFS concrete with water-binder ratio 0.44 and 0.5 using the extended Pickett model is shown in Figs. 25 and 26. The inputs of the model, i.e. the relative humidity, degree of saturation and elastic modulus of the BFS concrete are shown in Figs. 23 and 24. These inputs are simulated with HYMOSTRUC [48].

In Figs. 25 and 26 the predictions of the autogenous shrinkage of the BFS concrete mixture with the extended Pickett model are shown. It can be noticed that the calculated autogenous shrinkage is bigger than the measured result. More detailed discussion about the difference will be given in the following section.

5. Further discussion

In this paper, the extended Pickett model, which takes the creep behavior of the cement paste into consideration, was used to predict the autogenous shrinkage of Portland and BFS cement mortar and concrete. The comparison between the calculated and measured autogenous shrinkage of Portland and BFS cement mortar reveals that the extended Pickett model predicts the autogenous shrinkage of cement mortar with low aggregate volume fraction quite well.

For concrete with high aggregate fraction, the trend of the autogenous shrinkage can be predicted by using the extended Pickett model. However, it must be mentioned that the microcracking is not taken into consideration in the calculation with the extended Pickett model. Due to the restraining effect of the non-shrinking aggregate in concrete, cement paste in concrete is under tension. At the interface between the cement paste and inert particle, the tension is the largest. Due to the tension and low tensile strength of the cement paste, cracks perpendicular to the surface of the aggregate particle may form in the paste phase [50]. There is high

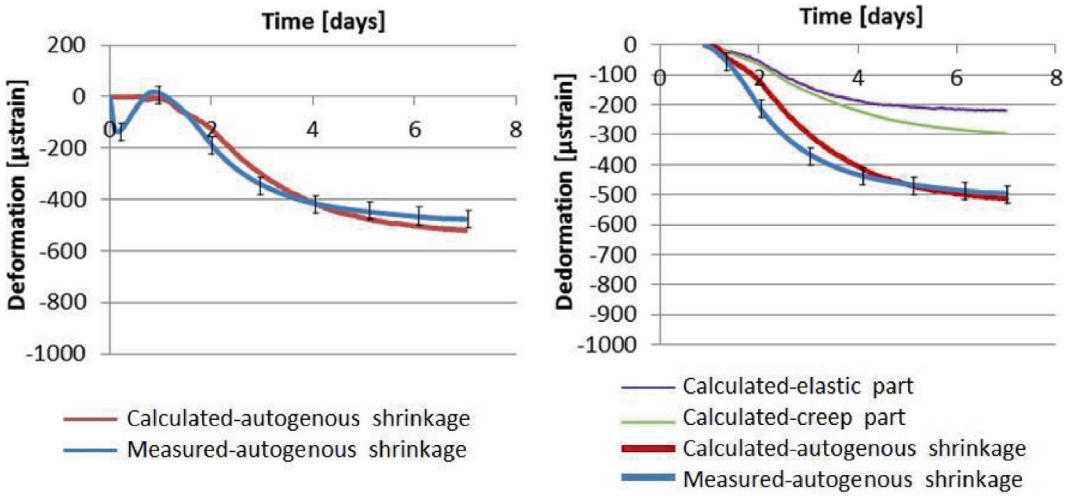

(a) Starting time: final setting time (b) Starting time: after maximum swelling

Fig. 16. Measured and calculated autogenous deformation of BFS cement mortar (30% sand) with water-binder ratio 0.3.

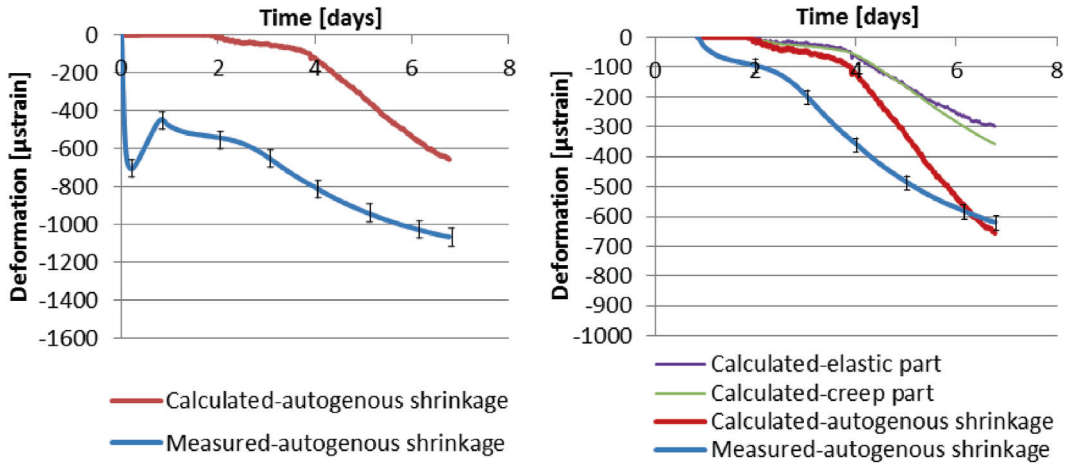

(a) Starting time: final setting time (b) Starting time: after maximum swelling

Fig. 17. Measured and calculated autogenous deformation of BFS cement paste with water-binder ratio 0.4 [36].

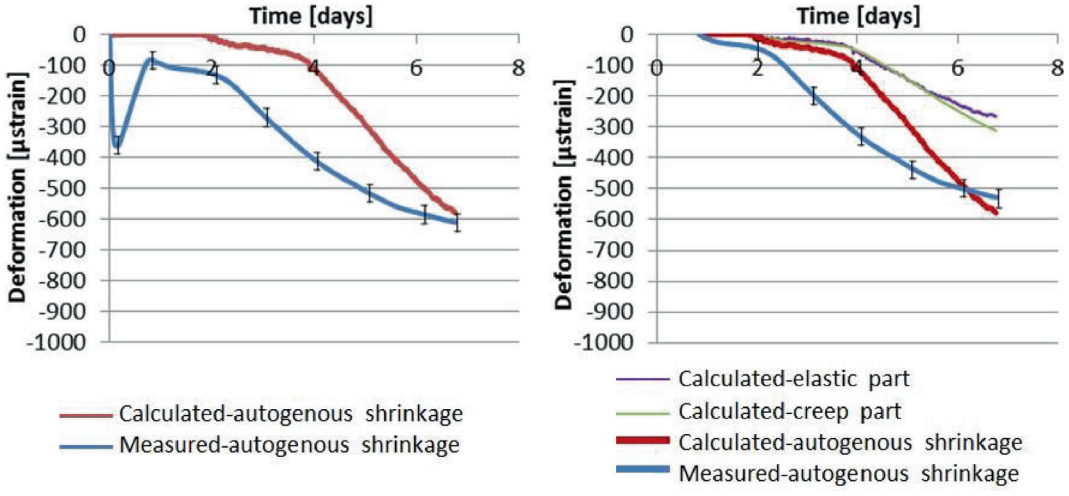

(a) Starting time: final setting time (b) Starting time: after maximum swelling

Fig. 18. Measured and calculated autogenous deformation of BFS cement mortar (10% sand) with water-binder ratio 0.4.

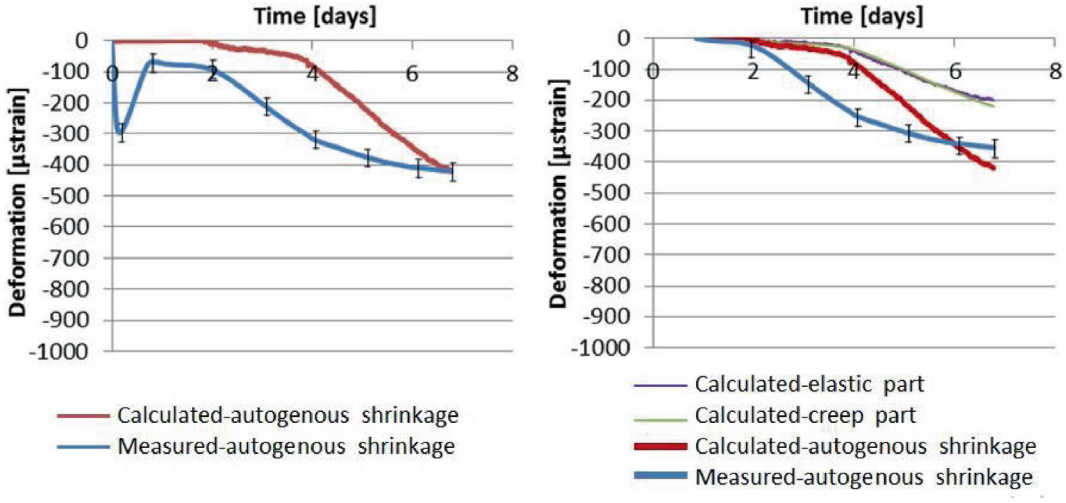

(a) Starting time: final setting time (b) Starting time: after maximum swelling

Fig. 19. Measured and calculated autogenous deformation of BFS cement mortar (30% sand) with water-binder ratio 0.4.

Table 2
Mixture composition of different concrete (% by weight).

Name	Reference	Binder		Mixture composition	
		Type I normal Portland cement (%)	CEM III/B 42.5 N (%)	w/b	Volume fraction of aggregate (%)
OPC 0.3	Zhang et al. 2003	100	0	0.3	71
BFS 0.44	Mors 2011	0	100	0.44	70
BFS 0.5	Mors 2011	0	100	0.5	70

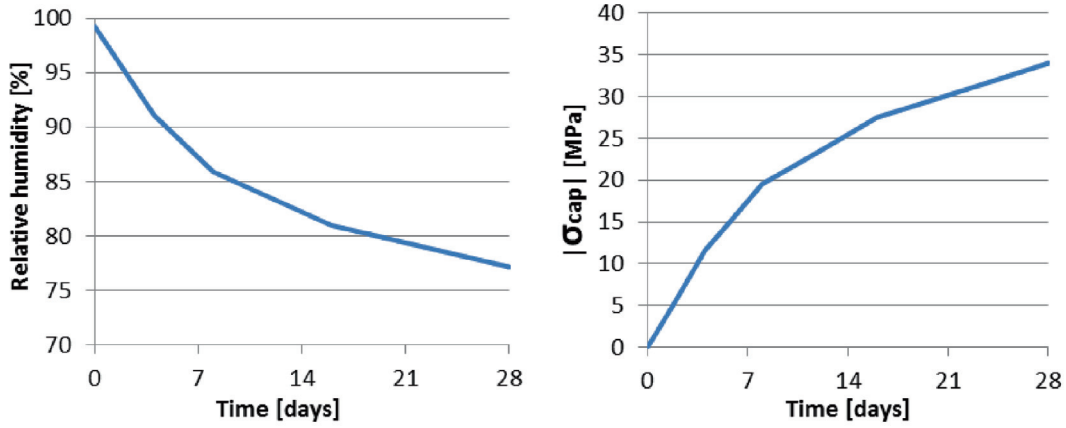

(a) Calculated relative humidity (with HYMOSTRUC) (b) Calculated capillary tension

Fig. 20. Calculated relative humidity and capillary tension of Portland cement concrete.

probability of microcracking in concrete after the first few days if the aggregate volume fraction is higher than 0.5 [6]. Microcracking can result in debonding between cement paste and sand particles and a reduction of the autogenous shrinkage. According to Maruyama [51] the value of calculated autogenous shrinkage of concrete may decrease by about 15% when the microcracking caused by internal restraint is taken into consideration. The adjusted autogenous shrinkage of Portland and BFS concretes by taking the microcracking into consideration (decrease by 15%) is indicated with the dashed line in Figs. 27, 28 and 29. From Fig. 27 it can be noticed that the measured and predicted shrinkage curves of Portland cement concrete are even closer. Fig. 28 and Fig. 29 show that the predicted autogenous shrinkage of BFS concrete is closer to the measured autogenous shrinkage after 14 days. However, it should be noticed that the effect of microcraking on shrinkage, i.e. 15% reduction, is estimation according to [51]. More attention should

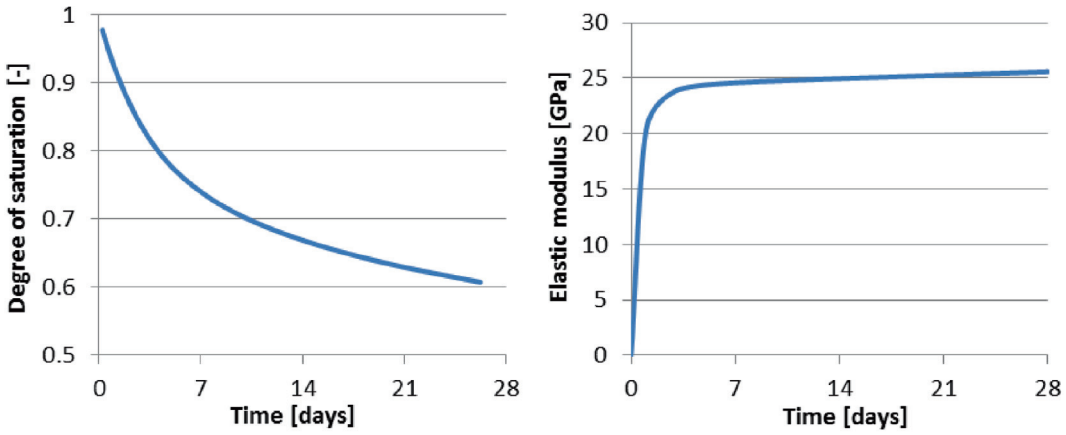

(a) Calculated degree of saturation (b) Calculated elastic modulus

Fig. 21. Calculated degree of saturation and elastic modulus (with HYMOSTRUC) of Portland cement concrete.

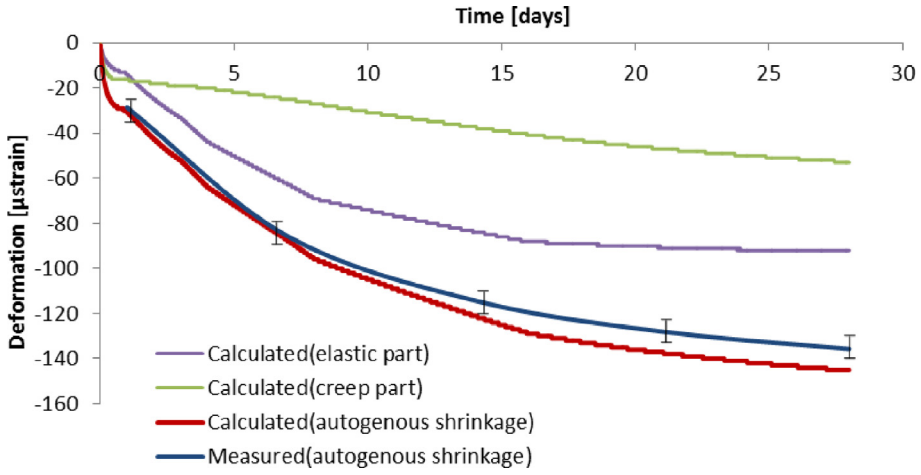

Fig. 22. Measured autogenous shrinkage [46] and calculated autogenous shrinkage of Portland cement concrete with the extended Pickett model.

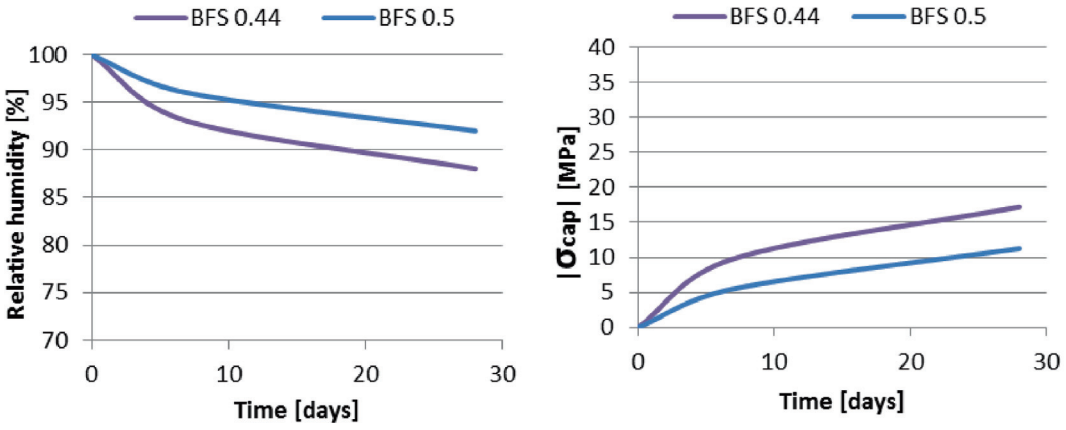

(a) Calculated relative humidity (with HYMOSTRUC) (b) Calculated capillary tension

Fig. 23. Calculated relative humidity and capillary tension of BFS concretes.

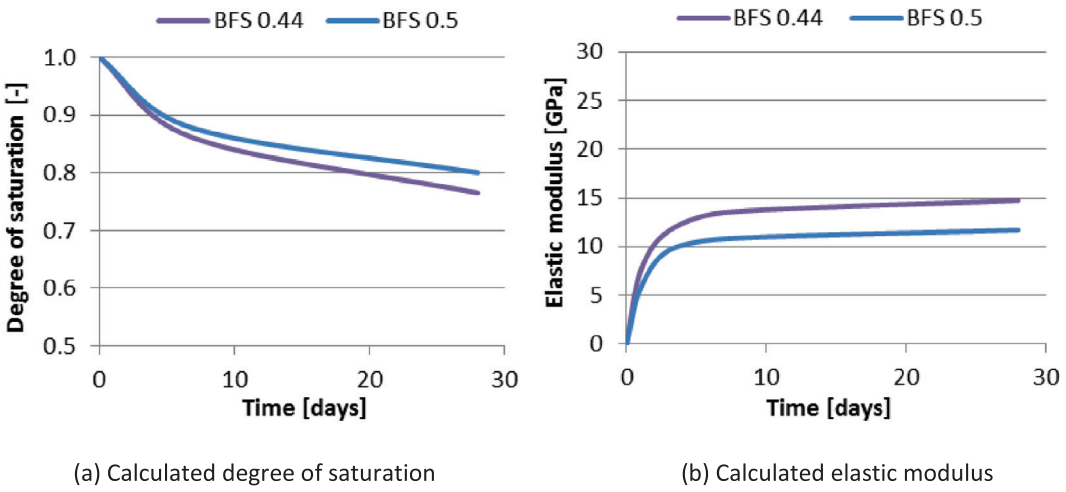

Fig. 24. Calculated degree of saturation and elastic modulus (with HYMOSTRUC) of BFS concretes.

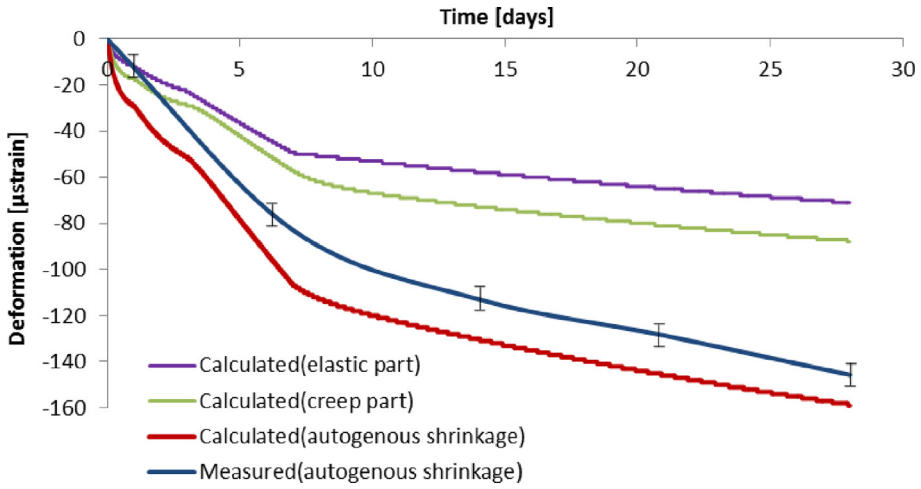

Fig. 25. Measured autogenous shrinkage of of BFS concrete with w/b 0.44 [47] and calculated autogenous shrinkage of BFS concrete with the extended Pickett model.

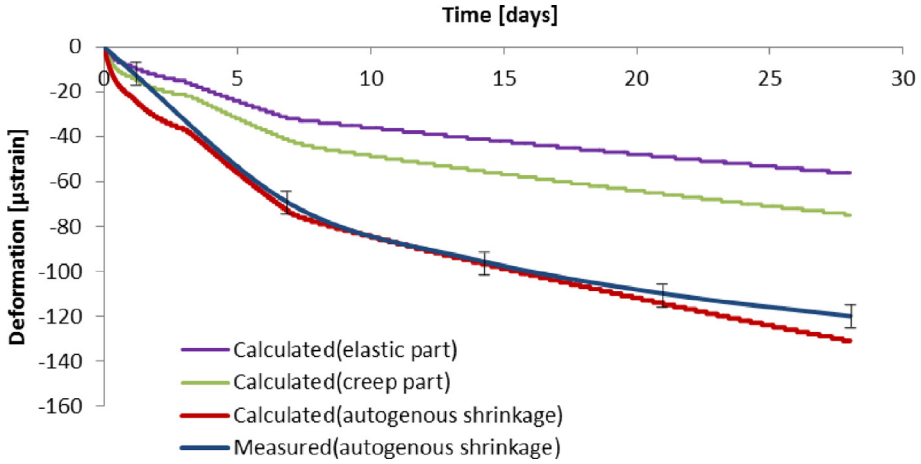

Fig. 26. Measured autogenous shrinkage of of BFS concrete with w/b 0.45 [47] and calculated autogenous shrinkage of BFS concrete with the extended Pickett model.

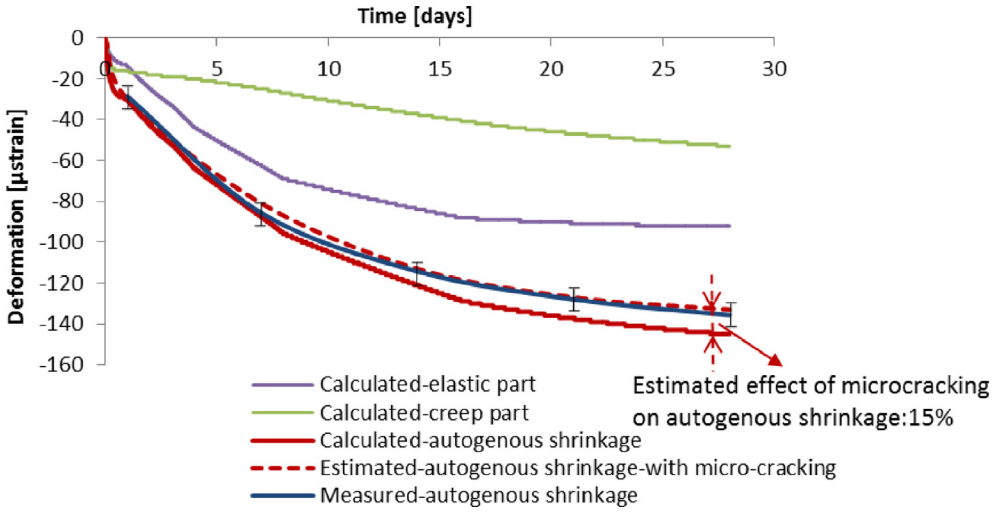

Fig. 27. Measured and adjusted calculated autogenous shrinkage of Portland cement concrete.

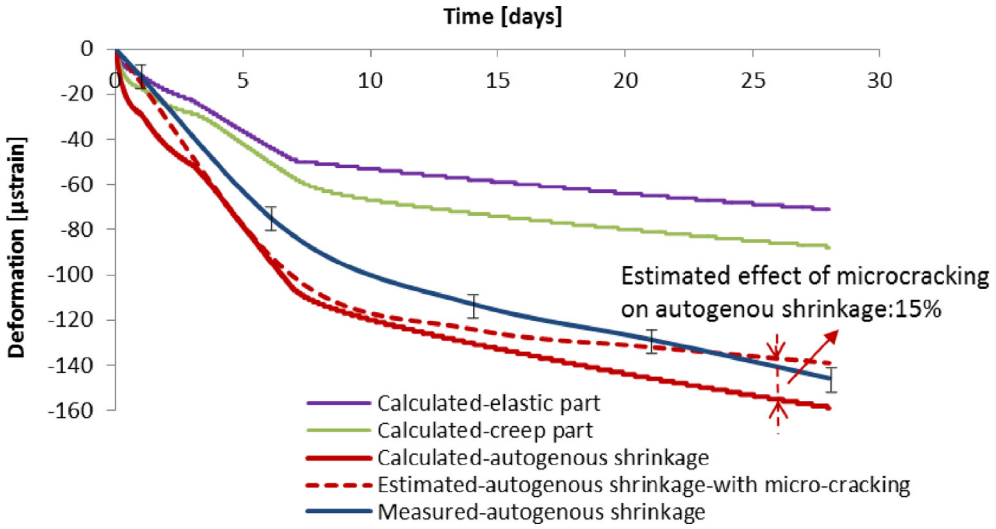

Fig. 28. Measured and adjusted calculated autogenous shrinkage of BFS concrete with w/b 0.44.

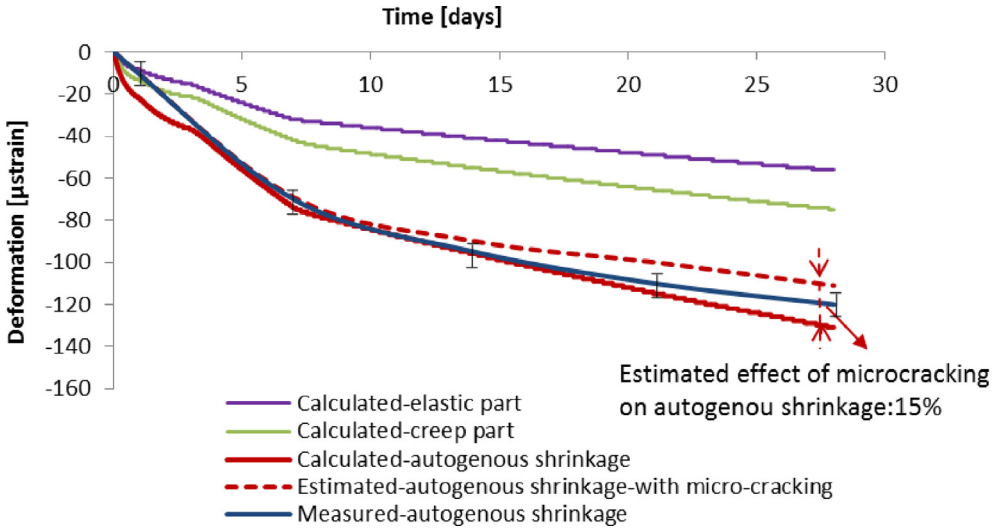

Fig. 29. Measured and adjusted calculated autogenous shrinkage of BFS concrete with w/b 0.5.

be paid to accurate quantification of the influence of microcracking on the autogenous shrinkage in the future research.

6. Concluding remarks

In this paper, Pickett model, which can be used to predict the restraining effect of aggregates on autogenous shrinkage, is extended to take the creep behaviour of cement paste into consideration. In the extended Pickett model, creep is simulated with formulas based on the activation energy theory. The predictions of autogenous shrinkage with the extended Pickett model were evaluated by comparing the calculated and measured autogenous shrinkage of Portland and BFS cement mortars. The comparison of the measured autogenous shrinkage with the autogenous shrinkage calculated with the extended Pickett model reveals that the extended Pickett model predicts the autogenous shrinkage of Portland and BFS cement mortars quite well.

The extended Pickett model was also used to predict the autogenous shrinkage of Portland and BFS concretes with high aggregate content. From the comparison between the calculated and measured results, it was found that the trend of autogenous shrinkage of the investigated concretes can be predicted by using the extended Pickett model. But the effect of microcracking is not taken into consideration in the extended Pickett model which will lead to bigger predicted autogenous shrinkage of concrete. After adjusting the calculated autogenous shrinkage for the effect of microcracking, the measured and predicted shrinkage curves of Portland cement concrete are even closer and the measured and predicted shrinkage curves of BFS cement concrete is closer after the first 14 days. However, it should also be noticed that the effect of microcraking on shrinkage, i.e. 15% reduction, is only an estimation according to the research of Maruyama. More attention should be paid to accurate quantification of the influence of microcracking on the autogenous shrinkage in the future research.

CRediT authorship contribution statement

Tianshi Lu: Conceptualization, Methodology, Investigation, Software, Writing - original draft. **Zhenming Li:** Methodology, Investigation, Writing - review & editing. **Hao Huang:** Writing - review & editing.

Declaration of Competing Interest

The authors declare that they have no known competing financial interests or personal relationships that could have appeared to influence the work reported in this paper.

Acknowledgement

Tianshi Lu, Zhenming Li and Hao huang would like to acknowledge the funding supported by the China Scholarship Council (CSC) and Delft University of Technology. Prof. Klaas van Breugel is gratefully acknowledged for his support and discussions of this study.

References

[1] E. Holt, Early age autogenous shrinkage of concrete, Julkaisija Utgivare Publisher. (2001).
[2] R. L'Hermite, Volume changes of concrete, Proceedings of fourth international symposium on the chemistry of cement, Washington, DC, (1960) 659–694.
[3] F.H. Wittmann, Surface Tension, Shrinkage and strength of hardened cement paste, Mater. Struct. 1 (6) (1968) 547–552.
[4] T.C. Powers, Session I: The thermodynamics of volume change and creep, Materiaux et Constructions 1 (6) (1968) 487–507.
[5] P. Lura, Autogenous deformation and internal curing of concrete. Ph.D. Thesis. (2003).
[6] T. Lu, Autogenous deformation of early age cement paste and mortar. Ph.D. Thesis. (2019).
[7] Z. Li, T. Lu, X. Liang, H. Dong, G. Ye, Mechanisms of autogenous shrinkage of alkali-activated slag and fly ash pastes, Cem. Concr. Res. 135 (2020) 106107, https://doi.org/10.1016/j.cemconres.2020.106107.
[8] K. van Breugel, Numerical modelling of volume changes at early ages - Potential, pitfalls and challenges, Mater. Struct. 34 (239) (2001) 293–301.
[9] T.C. Powers, Mechanisms of shrinkage and reversible creep of hardening cement paste, in Proc. Int. Symp. Structure of Concrete and its behaviour under load, Cem. & Concr. Ass., London, (1965) 319-344.
[10] E.A.B. Koenders, Simulation of volume changes in hardening cement-based materials. Ph.D. Thesis. (1997).
[11] Y. Wei, Modeling of autogenous deformation in cementitious materials, restraining effect from aggregate, and moisture warping in slabs on grade. Ph.D. Thesis. (2008).
[12] Z.C. Grasely, D.A. Lange, A.J. Brinks, D'Ambrosia, Modeling of autogenous shrinkage of concrete accounting for creep caused by aggregate restraint, self-desiccation and its importance in concrete technology, in: Proceedings of the Fourth International Research Seminar, 2005, pp. 1–20.
[13] B. Person, Creep and shrinkage of young or mature HPC. In Proc. 5th Int. Symp. on 'Utilization of high strength/high performance concrete', (1999) 1272-1281.
[14] D. Gawin, F. Pesavento, B.A. Schrefler, Modelling creep and shrinkage of concrete by means of effective stresses, Mater. Struct. 40 (6) (2007) 579–591.
[15] S.J. Lokhorst, K. van Breugel, Simulation of the effect of geometrical changes of the microstructure on the deformational behaviour of hardening concrete. Cem. Concr. Res. 27(1997) 1465-1479.
[16] R. Mabrouk, T. Ishiba, K. Maekawa, A unified solidification model of hardening concrete composite for predicting the young age behaviour of concrete, Cem. Concr. Res. 26 (2004) 453–461.
[17] R.L. Day, B.R. Gamble, The effect of changes in structure on the activation energy for the creep of concrete, Cem. Concr. Res. 13 (4) (1983) 529–540.
[18] M. Polivka, C.H. Best, Investigation of the problem of creep of concrete by Dorn's method, Springer, 39th Annual Meeting of the Highway Research Board, 1960.
[19] F. Wittmann, Kriechverformung des Betons unter statischer und unter dynamischer Belastung, Rheol. Acta 10 (3) (1971) 422–428.
[20] G. Pickett, Effect of aggregate on shrinkage of concrete and a hypothesis concerning shrinkage, ACI J. 52 (5) (1956) 581–590.
[21] R. Defay, I. Prigogine, Surface Tension and Adsorption, Green & Co Ltd, London, Longmans, 1966.
[22] O.M. Jensen, Autogenous deformation and RH-change – self-desiccation and self-desiccation shrinkage (in Danish), TR 284/93, Building Materials Laboratory, The Technical University of Denmark, Lyngby, Denmark (1993).
[23] Hans-Jürgen Butt, Michael Kappl, Normal capillary forces, Adv. Colloid Interface Sci. 146 (1-2) (2009) 48–60.
[24] William G Gray, Bernhard A Schrefler, Thermodynamic approach to effective stress in partially saturated porous media, Eur. J. Mech. A/Solids 20 (4) (2001) 521–538.
[25] T.C. Powers, T.L. Brownyard, Studies of the physical properties of hardened Portland cement paste (9 parts), J Amer Concr Inst 43 (Oct. 1946 to April 1947), Bulletin 22, Research Laboratories of the Portland Cement Association, Chicago (1948).
[26] M.M. Alam, M.K. Borre, I.L. Fabricius, K. Hedegaard, B. Røgen, Z. Hossain, A.S. Krogsbøll, Biot's coefficient as an indicator of strength and porosity reduction: Calcareous sediments from Kerguelen Plateau, J. Petrol. Sci. Eng. 70 (2010) 282–297.
[27] L.F. Nielsen, A research note on sorption, pore size distribution, and shrinkage of porous materials, TR 245/91, Building Materials Laboratory, The Technical University of Denmark, Lyngby, Denmark (1991).
[28] S. Timoshenko, J.N. Goodier, Theory of Elasticity, 2nd Edition., McGraw-Hill Book Co., Inc.,, New York, 1951.
[29] P. Klug, F. Wittmann, Activation energy of creep of hardened cement paste, Matériaux et Constr. 2 (1) (1969) 11–16.
[30] Folker Wittmann, Kriechen bei gleichzeitigem Schwinden des Zementsteins, Rheol. Acta 5 (3) (1966) 198–204.
[31] F. Wittmann, P. Klug, Zum zeitlichen Verlauf des Kriechens von Zementstein und Beton, Rheol. Acta 7 (1) (1968) 93–95.
[32] G.A. Hirst, A.M. Neville, Activation energy of creep of concrete under short-term static and cyclic stresses, Mag. Concr. Res. 29 (98) (1977) 13–18.
[33] T.C. Hansen, K.E.C. Nielsen, Influence of aggregate properties on concrete shrinkage, ACI J. 62 (7) (1965) 783–794.
[34] T.Y. Zhu, Some Useful Numbers on the Engineering Properties of Materials (Geologic and Otherwise). GEOL 615, Department of Geophysics. (2012).
[35] C. ASTM, Standard practice for mechanical mixing of hydraulic cement pastes and mortars of plastic consistency. In American Society for Testing and Materials. (1999). 305-99.
[36] T. Lu, Z. Li, K. van Breugel, Modelling of autogenous shrinkage of hardening cement paste, Constr. Build. Mater. 264 (2020) 120708.
[37] Standard, A. S. T. M. "Standard test method for autogenous strain of cement paste and mortar." ASTM C-1698 (2009).
[38] NEN-EN 196-3, Methods of Testing Cement. Part 3: Determination of Setting Times and Soundness (2005).
[39] C.W. Miao, Q. Tian, W. Sun, J.P. Liu, Water consumption of the early-age paste and the determination of "time-zero" of self-desiccation shrinkage, Cem. Concr. Res. 37 (2007) 1496–1501.

[40] A. Bentur, Terminology and definitions, in: K. Kovler, A. Bentur (Eds.). International RILEM Conference on Early Age Cracking in Cementitious Systems—EAC, RILEM TC181-EAS, Haifa (2002) 13–20.
[41] G. Sant, F. Rajabipour, P. Lura, J. Weiss, Examining time-zero and early age expansion in pastes containing shrinkage reducing admixtures (SRA's), In Proc., 2nd RILEM Symp. on Advances in Concrete through Science and Engineering, 2006.
[42] H. Huang, G. Ye, Examining the "time-zero" of autogenous shrinkage in high/ultra-high performance cement pastes, Cem. Concr. Res. 97 (2017) 107–114.
[43] Ø. Bjøntegaard, Thermal dilatation and autogenous deformation as driving forces to self-inducedstresses in high performance concrete, Ph.D. Thesis (1999).
[44] Y. Wei, S. Liang, X. Gao, Simulation of porosity effect on mechanical and creep properties of cement paste at microscale, Poromechanics VI (2017) (2017) 1099–1107.
[45] Z. Hu, Prediction of autogenous shrinkage in fly ash blended cement systems, Ph.D. Thesis (2017).
[46] M.H. Zhang, C.T. Tam, M.P. Leow, Effect of water-to-cementitious materials ratio and silica fume on the autogenous shrinkage of concrete, Cem. Concr. Res. 33 (10) (2003) 1687–1694.
[47] R.M. Mors, Autogenous shrinkage of cementitious materials containing BFS, Master thesis (2011).
[48] K. van Breugel, Simulation of hydration and formation of structure in hardening cement-based materials, Ph.D. Thesis (1991).
[49] S.J. Lokhorst, Deformational behaviour of concrete influenced by hydration related changes of the microstructure. University of Techn., Fac. of Civil Engineering, Concrete Structures (1998).
[50] P. Goltermann, Mechanical predictions on concrete deterioration. Part 1: eigenstresses in concrete, ACI Mater. J. 91 (6) (1994) 543–550.
[51] I. Maruyama, S. Kameta, M. Suzuki, R. Sato, Cracking of high strength concrete around deformed reinforcing bar due to shrinkage. In Int. RILEM-JCI Seminar on Concrete Durability and Service Life Planning. RILEM Publications SAR L Ein-Bokek, Israel. (2006) 104-111.